

Thermodynamics of warm axionic Abelian gauge inflation

Xi-Bin Li(李喜彬) and Yan-Ling Wu(武燕玲)
Citation: Chin. Phys. B, 2023, 32 (**11**): 119801. DOI: 10.1088/1674-1056/acea6a
Journal homepage: http://cpb.iphy.ac.cn; http://iopscience.iop.org/cpb

What follows is a list of articles you may be interested in

Inflationary dynamics in the braneworld scenarios

Zhang Kai-Yuan (张开源), Wu Pu-Xun (吴普训), Yu Hong-Wei (余洪伟)
Chin. Phys. B, 2013, 22 (**5**): 059801. DOI: 10.1088/1674-1056/22/5/059801

Spontaneous symmetry breaking vacuum energy in cosmology

Zhou Kang(周康), Yue Rui-Hong(岳瑞宏), Yang Zhan-Ying(杨战营), and Zou De-Cheng(邹德成)
Chin. Phys. B, 2012, 21 (**7**): 079801. DOI: 10.1088/1674-1056/21/7/079801

Cosmological applications in Kaluza–Klein theory

M. I. Wanas, Gamal G. L. Nashed, and A. A. Nowaya
Chin. Phys. B, 2012, 21 (**4**): 049801. DOI: 10.1088/1674-1056/21/4/049801

Thermodynamics of warm axionic Abelian gauge inflation

Xi-Bin Li(李喜彬)[1,2,†] and Yan-Ling Wu(武燕玲)[1,2]

[1] *College of Physics and Electronic Information, Inner Mongolia Normal University, Hohhot* 010022, *China*
[2] *Inner Mongolia Key Laboratory for Physics and Chemistry of Functional Materials, Inner Mongolia Normal University, Hohhot* 010022, *China*

(Received 28 May 2023; revised manuscript received 3 July 2023; accepted manuscript online 26 July 2023)

Inflationary spectral index from the Langevin equation is calculated under the frame of warm inflationary scenario with inflaton interacting with $U(1)$ gauge fields through the Chern–Simons coupling $\propto \phi F_{\mu\nu}\tilde{F}^{\mu\nu}/f$. Under the strong dissipative condition, the spectral index is calculated in terms of the ratio of Hubble parameter to temperature H/T. Then relation between H/T and other cosmic parameters is analytically expressed, based on which a spectral index related to the Chern–Simons coupling strength is further obtained. Numerical results show that cosmic temperature T closes to a constant during inflation and decreases after inflation without a reheating process. Meanwhile, the ratio H/T tends to a constant if the gauged coupling constant is less than a threshold. This phenomenon shows that cosmic temperature may be an important physical parameter with a special value and adiabatic approximation still holds. We obtain the estimate $H/T \leq 0.3377$ during inflation from Planck data and other constraint conditions.

Keywords: axion inflation, thermodynamics

PACS: 98.80.–k, 98.80.Bp, 98.80.Es, 05.70.Ce **DOI:** 10.1088/1674-1056/acea6a

1. Introduction

The inflation model is established to overcome some defects of the standard big bang theory.[1–4] This model has successfully answered the problems like the formation of cosmic large-scale structure[5–7] and the anisotropy of microwave background,[8–10] but come problems that, in cold inflation, the inflaton does not interact with other fields and the Universe is required a reheating process after inflation when the scalar field reaches the bottom of the potential and starts oscillating. However, this puts forward higher requirements for the potential and the reheating itself may also face some problems. Furthermore, the latest Planck data ruled out many forms of inflation potentials, including the quadratic and quartic potentials, both widely accepted from the perspective of particle physics.[11]

On the other hand, the warm inflation model was proposed as a candidate scenario to solve the problems in cold inflation.[12,13] Warm inflation has been studied for a long time as a possible and realizing model.[14–16] In warm inflationary scenario, the evolution of the inflaton field can be properly determined in the context of the in-in formalism, or Schwinger closed-time path functional formalism.[17] This formalism leads an stochastic differential equation which contains a dissipative term and a Gaussian stochastic noise term as a type of generalized Langevin-like equation of motion.[18,19]

Inflation driven by an axion-like particle, often dubbed as natural inflation,[20,21] is one of the most well-motivated models of inflation to reheat the Universe.[22] In axion inflation the flatness of the potential is guaranteed by the shift symmetry and ensures a potential periodic. However, this model in cold inflation is strongly disfavored by Planck 2018 data.[23] Another objective in cold inflation is the realization of an exponential production of radiation in order to overcome the exponential dilution without spoiling the slow-roll stage. For this purpose, the thermalized axion inflation model is introduced, in which the gauge fields A_μ simply couple to an axion-like field ϕ and the gauge fields are considered as the thermal bath.[24] In this model, inflation often follows a kination era where the Universe is then dominated by the kinetic energy of inflaton, which suppresses the generation of radiation field and may need a long time to transit from inflation to radiation domination. On the contrary, warm inflation allows a dissipative term $\Upsilon\dot{\phi}$ in the equation of motion of inflaton, which represents the decay from inflaton to thermal bath. Thus the combination of axion inflation and warm inflation is a reasonable arrangement, and this model is also called the minimal warm inflation.[25–28] Warm axion inflation allows inflaton to decay into gauge field at any time and make it possible to analyze the thermodynamics of the early Universe. The strong coupling (or strong dissipative effect) can effectively restrain the conversion to kinetic energy, thus avoiding the kination era and realizing the exponential production of thermal bath. Most importantly, warm inflationary scenario makes the pseudoscalar inflation model compatible with the Planck 2018 results.[29]

So far, there have been enough discussions on the self consistency and rationality of the warm inflation theory, but further research on thermal effect, directly related to the thermal effect, still needs to be conducted in depth. The thermal quantity T make it possible to provide a detailed analysis on the thermal properties during and after inflation. In this paper,

[†]Corresponding author. E-mail: lxbimnu@imnu.edu.cn

© 2023 Chinese Physical Society and IOP Publishing Ltd

by starting from the Langevin equation, inflationary spectral index is analytically calculated in the model of warm axionic Abelian gauge inflation. The equation about the ratio of Hubble parameter to cosmic temperature H/T is obtained, then H/T and T are numerical solved. This work provides a new scheme for the study of the thermodynamics in the early Universe, especially the evolution of temperature, and also provides a new idea for the discussion of the reheating process.

The organization of this paper is as follows: In Section 2, the spectral index is calculated from the Langevin equation in the framework of warm axion inflation. In Section 3, equations related to thermal effect, especially the cosmic temperature T, are calculated theoretically. Then, numerical results are obtained in Section 3 and discussed in detail. Finally, in Section 4, we conclude our work and give some outlooks about our further research.

2. Spectral index of minimal warm inflation

We consider the model described by the following matter Lagrangian:[30]

$$\mathcal{L}_m = -\frac{1}{2}\partial_\mu\phi\partial^\mu\phi - V(\phi) - \frac{1}{4}F_{\mu\nu}F^{\mu\nu} - \frac{g^2}{4}\frac{\phi}{f}F_{\mu\nu}\tilde{F}^{\mu\nu}, \quad (1)$$

where ϕ is the (axion)-inflaton regarded as a scalar field and $V(\phi)$ is the potential. Gauge field strength tensor is defined by $F_{\mu\nu} = \partial_\mu A_\nu - \partial_\nu A_\mu$. The gauge field A_μ couples with the inflaton through the Chern–Simons term, with the dual tensor $\tilde{F} = \eta^{\mu\nu\rho\sigma}F_{\mu\nu}/(2\sqrt{-g})$, where $\eta^{\mu\nu\rho\sigma}$ is the Levi–Civita tensor in Minkowski spacetime.

2.1. Perturbed dynamics

In the warm inflation model, the dynamical equation of inflaton is described by an additional dissipative term Υ. We define a new variable as the ratio of dissipative coefficient to the Hubble parameter $Q = \Upsilon/3H$, such that

$$\ddot{\phi}_0 + 3H(1+Q)\dot{\phi}_0 + V_{,\phi} = 0, \quad (2)$$

$$\delta\ddot{\phi} + 3H(1+Q)\delta\dot{\phi} - \frac{1}{a^2}\nabla^2\delta\phi + V_{,\phi\phi}\,\delta\phi = \xi. \quad (3)$$

The strong dissipative regime of warm inflation[25] makes it possible to lead a rapid production of radiation, so in this paper we work under a strongly dissipative condition, i.e., $Q \gg 1$. The symbol ϕ_0 means the background inflaton, $\delta\phi$ means the perturbed field formulated by the Langevin equation. The dots denote the derivatives with respect to cosmic time $t(\dot{\phi} = \frac{\mathrm{d}\phi}{\mathrm{d}t})$ and $V_{,\phi}$ denotes the derivatives on potential V with respect to inflation field $(V_{,\phi} = \frac{\mathrm{d}V}{\mathrm{d}\phi})$; ξ in the Langevin equation (3) is the fluctuation term describing a Gaussian thermal noise effect, which satisfies the fluctuation–dissipation relation

$$\langle\xi(\boldsymbol{x},t)\xi^*(\boldsymbol{x}',t')\rangle = 2a^{-3}\Upsilon k_{\mathrm{B}}T\delta^3(\boldsymbol{x}-\boldsymbol{x}')\delta(t-t'), \quad (4)$$

whose Fourier transformation reads

$$\langle\xi_T(\boldsymbol{k},t)\xi_T^*(\boldsymbol{k}',t')\rangle = 2(2\pi^3)\Upsilon k_{\mathrm{B}}Ta^{-3}\delta^3(\boldsymbol{k}-\boldsymbol{k}')\delta(t-t'). \quad (5)$$

The most-motivated model for axion-like particles is the natural potential given by

$$V(\phi) = \Lambda^4\left[1-\cos\left(\frac{\phi}{f}\right)\right]. \quad (6)$$

Given an interaction Lagrangian density like $\mathcal{L}_{\mathrm{int}} = -f(\phi)g(X)$, where X is an arbitrary field coupling with ϕ, the dissipative coefficient is analytically expressed as[31]

$$-\mathrm{i}\frac{\mathrm{d}f(\phi)}{\mathrm{d}\phi}\int \mathrm{d}^4x'\theta(t-t')[f(\phi(x')) - f(\phi(x))] \times\langle[g(X(x)), g(X(x'))]\rangle \approx \Upsilon\dot{\phi}. \quad (7)$$

Lagrangian (1) leads an inflaton ϕ independent dissipative coefficient[32]

$$\Upsilon = g^4\frac{m_\phi^3}{64\pi f^2} = \alpha_g\frac{m_\phi^3}{f^2}, \quad (8)$$

with $m_\phi = \Lambda^2/f^2$ and $\alpha_g = g^4/64\pi$ for the convenience of expression. Thermal effects also lead to an additional term describing the energy density of radiation in Friedman equation:

$$H^2 = \frac{1}{3M_{\mathrm{p}}^2}\left(\frac{1}{2}\dot{\phi}^2 + V + \rho_{\mathrm{r}}\right), \quad (9)$$

where the Planck mass is defined as $M_{\mathrm{p}}^2 = 1/(8\pi G)$.

To characterize the dynamical and thermal properties of inflation, it is necessary to define three slow-roll parameters

$$\varepsilon_{\mathrm{H}} \equiv -\frac{\dot{H}}{H^2} \ll 1, \quad (10a)$$

$$\eta \equiv M_{\mathrm{p}}^2\frac{V_{,\phi\phi}}{V} \ll 1+Q, \quad (10b)$$

$$\beta \equiv M_{\mathrm{p}}^2\frac{\Upsilon_{,\phi}V_{,\phi}}{\Upsilon V} \ll 1+Q. \quad (10c)$$

The first slow-roll parameter in Eq. (10) means a nearly exponential expansion of the early Universe, the second one means the requirement on the flatness of potential in terms of inflaton, and the third one is required from the restriction of dissipative coefficient and potential on the inflaton derivative, namely the adiabatic approximation. Here, independent dissipative coefficient ϕ means $\beta = 0$. In the following calculations, another more important slow-roll parameter $\varepsilon \equiv Q\varepsilon_{\mathrm{H}}$ will be used by satisfying the approximation

$$\frac{\varepsilon}{1+Q} \ll 1. \quad (10d)$$

Another way to describe the new parameter is via the derivative on potential

$$\varepsilon \approx (1+Q)\varepsilon_{\mathrm{H}} = \frac{M_{\mathrm{p}}^2}{2}\left(\frac{V_{,\phi}}{V}\right)^2. \quad (10e)$$

The fact that potential contributes the most of the total energy density during inflation helps us to simplify the above dynamical equations to

$$3H(1+Q)\dot{\phi} \approx -V_{,\phi}\,. \tag{11}$$

Introducing the variable $z = k/(aH)$, together with the partial derivative with respect to cosmic time $\frac{\partial}{\partial t} = -(1-\varepsilon)zH\frac{\partial}{\partial z}$ and relation $\frac{1}{H}\frac{\mathrm{d}H}{\mathrm{d}z} = -\varepsilon$, Eq. (3) in momentum space becomes

$$\begin{aligned}&\delta\phi'' + \frac{1}{z}\Big(1 - 2\frac{3+3Q-3\varepsilon}{2}\Big)\delta\phi' \\ &+ \Big(1 + \frac{3(\eta - \beta Q/(1+Q))}{z^2}\Big)\delta\phi = \frac{1}{z^2H^2}\xi,\end{aligned} \tag{12}$$

where the primes denote the derivatives with respect to variable z. The definition of z gives the identity

$$\int_{t_i}^{t} H\mathrm{d}t_1 = \ln\Big(\frac{k}{zHa_i}\Big), \tag{13}$$

with scale factor a_i at instant t_i of inflation. Inserting the above equation into a delta function $\delta(\int_{t_i}^{t} H\mathrm{d}t_1 - \int_{t_i}^{t'} H\mathrm{d}t_2) = \delta(\ln(z'H'/zH))$ and using the property of delta function $\delta(f(x)) = \sum_{\{x_0\}}\frac{\delta(x-x_0)}{|f'(x_0)|}$, where $\{x_0\}$ are the zero points of function $f(x)$, we can obtain the relation $\delta(t-t') = zH\delta(z - z'H'/H) = zH\delta(z-z')$. The last step has used the fact $H'/H = 1+\varepsilon(t)-\varepsilon(t') = 1$ because of the delta function $\delta(t-t')$. Thus the fluctuation–dissipation relation (5) becomes

$$\begin{aligned}&\langle\xi_i(\boldsymbol{k},z)\xi_j^*(\boldsymbol{k}',z')\rangle \\ &= 2(2\pi^3)\Upsilon k_{\mathrm{B}}T\frac{H^4z^4}{k^3}\delta^3(\boldsymbol{k}-\boldsymbol{k}')\delta(z-z').\end{aligned} \tag{14}$$

Applying Green's function method, the solution of differential equation (12) is[33]

$$\delta\phi_1(\boldsymbol{k},z) = \int_z^{\infty}\mathrm{d}z' G(z,z')\frac{1}{z'^2H^2}\xi_1(\boldsymbol{k},z') \tag{15}$$

with Green's function

$$\begin{aligned}G(z,z') = \frac{z^{\alpha}}{z'^{\alpha}}\frac{1}{2/\pi z'}&[J_{\nu}(z)N_{\nu}(z') \\ &- J_{\nu}(z')N_{\nu}(z)]\theta(z'-z).\end{aligned} \tag{16}$$

In the above equation, $J_{\nu}(z)$ is the Bessel function of ν-th order and $N_{\nu}(z)$ is the Neumann function with parameters

$$\alpha = \frac{3}{2}(1+Q-\varepsilon), \tag{17}$$

$$\begin{aligned}\nu &= \sqrt{\alpha^2 + \frac{3\beta Q}{1+Q} - 3\eta} \\ &\approx \alpha - \frac{\eta}{1+Q} + \frac{\varepsilon\eta}{(1+Q)^2}.\end{aligned} \tag{18}$$

Due to the solution of perturbed field (15) and the fluctuation–dissipation relation (5), the correlation function of perturbed field reads

$$\begin{aligned}\langle\delta\phi(\boldsymbol{k},z)\delta\phi(\boldsymbol{k}',z')\rangle &= (2\pi)^3k^{-3}\delta^3(\boldsymbol{k}-\boldsymbol{k}') \\ &\times 2k_{\mathrm{B}}T\Upsilon\int_{z_m}^{\infty}\mathrm{d}z''G(z,z'')G(z',z''),\end{aligned} \tag{19}$$

with $z_m = \min(z,z')$. The slow-roll limit also indicates $\alpha-\nu\sim 0$, so $z^{\alpha}J_{\nu}(z)\to 0$ and $z^{\alpha}N_{\nu}(z)$ tends to a constant on the large scale limit $z\to 0$. Then one can ignore the integrals containing Neumann function $N_{\nu}(z')$ and needs only to consider the term $\int_z^{\infty}\mathrm{d}z'z'^{2-2\alpha}J_{\nu}^2(z')$. With the help of Weber–Schafheitlin integrals[34] and the approximation $N_{\nu}(z)\approx -\frac{\Gamma(\nu)}{\pi}(\frac{2}{z})^{\nu}$ as $z\to 0^+$, the correlation function (19) expresses

$$\begin{aligned}&\langle\delta\phi(\boldsymbol{k},z)\delta\phi(\boldsymbol{k}',z')\rangle|_{z'=z} \\ &\approx(\pi^3/2)k^{-3}\delta^3(\boldsymbol{k}-\boldsymbol{k}')\Upsilon T2^{3-2(\alpha-\nu)}z^{2(\alpha-\nu)} \\ &\times\frac{\Gamma^2(\nu)\Gamma(\frac{3}{2}-(\alpha-\nu))\Gamma(2\alpha-2)}{\Gamma^2(\alpha-\frac{1}{2})\Gamma(\alpha+\nu-\frac{3}{2})},\end{aligned} \tag{20}$$

from which we obtain the power spectrum of curvature perturbation:

$$\Delta_R^2(\boldsymbol{k}) = \Big(\frac{H}{\dot{\phi}}\Big)^2\frac{k^3}{2\pi^2}\int\mathrm{d}^3k'\langle\delta\phi(\boldsymbol{k},z)\delta\phi(\boldsymbol{k}',z)\rangle. \tag{21}$$

2.2. Spectral index

The spectral index of curvature perturbation is defined as

$$n_{\mathrm{s}} - 1 = \frac{\mathrm{d}\ln\Delta_R^2}{\mathrm{d}\ln k}. \tag{22}$$

Noticing the relation of frozen scale in warm inflation model $\mathrm{d}\ln k = (1+Q)\mathrm{d}N$ with $\mathrm{d}N = H\mathrm{d}t$, we can get the following expressions in terms of the derivative of N:

$$\frac{\mathrm{d}\ln H}{\mathrm{d}N} = -\varepsilon_{\mathrm{H}}, \tag{23a}$$

$$\frac{\mathrm{d}\ln Q}{\mathrm{d}N} = \varepsilon_{\mathrm{H}}, \tag{23b}$$

$$\frac{\mathrm{d}\ln\eta}{\mathrm{d}N} = -\frac{\eta-2\varepsilon}{1+Q}, \tag{23c}$$

$$\frac{\mathrm{d}\ln\varepsilon}{\mathrm{d}N} = -\frac{2(\eta-2\varepsilon)}{1+Q}. \tag{23d}$$

Combining Eqs. (23b) and (23c), we then have

$$\frac{\mathrm{d}}{\mathrm{d}N}\frac{\eta}{1+Q} = -\frac{\eta(\eta-2\varepsilon+\varepsilon_{\mathrm{H}})}{(1+Q)^2}. \tag{23e}$$

The derivative variables in Eq. (23e) are regarded as the second order of slow-roll parameters. We still have

$$\begin{aligned}\frac{\mathrm{d}\ln(H^2/\dot{\phi}^2)}{\mathrm{d}N} &= \frac{\mathrm{d}\ln[(1+Q)^2/(2M_{\mathrm{p}}^2\varepsilon)]}{\mathrm{d}N} \\ &= \frac{2Q}{1+Q}\frac{\mathrm{d}\ln Q}{\mathrm{d}N} + \frac{2(\eta-3\varepsilon)}{1+Q},\end{aligned} \tag{23f}$$

$$\frac{\mathrm{d}\ln\Upsilon k_{\mathrm{B}}T}{\mathrm{d}N} = \frac{\mathrm{d}\ln T}{\mathrm{d}N}, \tag{23g}$$

$$\frac{\mathrm{d}\ln 2^{-2(\alpha-\nu)}}{\mathrm{d}N} = 2\ln 2\frac{\mathrm{d}}{\mathrm{d}N}\frac{\eta}{1+Q}, \tag{23h}$$

$$\frac{\mathrm{d}\ln z^{2(\alpha-\nu)}}{\mathrm{d}\ln k}=\frac{2\eta}{1+Q}-\frac{2\varepsilon\eta}{(1+Q)^2}. \tag{23i}$$

The spectral index contains the derivative on the Gamma function $\frac{\mathrm{d}\ln\Gamma(a+\varepsilon)}{\mathrm{d}z}=\psi(a+\varepsilon)\frac{\mathrm{d}\varepsilon}{\mathrm{d}z}$, where $\psi(z)=\frac{\mathrm{d}\ln\Gamma(z)}{\mathrm{d}z}$ is the Psi function. Then we have

$$\begin{aligned}&\frac{\mathrm{d}\ln\Gamma^2(\nu)}{\mathrm{d}N}\\&=3\psi\Big(\frac{3}{2}+\frac{3}{2}Q\Big)\Big(\frac{\mathrm{d}Q}{\mathrm{d}N}-\frac{\mathrm{d}\varepsilon}{\mathrm{d}N}-\frac{2}{3}\frac{\mathrm{d}}{\mathrm{d}N}\frac{\eta}{1+Q}\Big),\end{aligned} \tag{24a}$$

$$\frac{\mathrm{d}\ln\Gamma(\frac{3}{2}-(\alpha-\nu))}{\mathrm{d}N}=-\psi\Big(\frac{3}{2}\Big)\frac{\mathrm{d}}{\mathrm{d}N}\frac{\eta}{1+Q}, \tag{24b}$$

$$\frac{\mathrm{d}\ln\Gamma(2\alpha-2)}{\mathrm{d}N}=3\psi(1+3Q)\Big(\frac{\mathrm{d}Q}{\mathrm{d}N}-\frac{\mathrm{d}\varepsilon}{\mathrm{d}N}\Big), \tag{24c}$$

$$-\frac{\mathrm{d}\ln\Gamma^2(\alpha-\frac{1}{2})}{\mathrm{d}N}=3\psi\Big(1+\frac{3}{2}Q\Big)\Big(\frac{\mathrm{d}Q}{\mathrm{d}N}-\frac{\mathrm{d}\varepsilon}{\mathrm{d}N}\Big), \tag{24d}$$

$$\begin{aligned}&-\frac{\mathrm{d}\ln\Gamma(\alpha+\nu-\frac{3}{2})}{\mathrm{d}N}\\&=3\psi\Big(\frac{3}{2}+3Q\Big)\Big(\frac{\mathrm{d}Q}{\mathrm{d}N}-\frac{\mathrm{d}\varepsilon}{\mathrm{d}N}-\frac{1}{3}\frac{\mathrm{d}}{\mathrm{d}N}\frac{\eta}{1+Q}\Big).\end{aligned} \tag{24e}$$

By collecting the above formulas, we can continue to simplify the expressions. The strong dissipative effect $Q\gg1$ and the limiting form $\psi(z)\sim\ln z-\frac{1}{2z}$ [34] as $z\gg1$ lead to approximate results

$$\begin{aligned}&\psi\Big(\frac{3}{2}+\frac{3}{2}Q\Big)+\psi(1+3Q)-\psi\Big(1+\frac{3}{2}Q\Big)\\&-\psi\Big(\frac{3}{2}+3Q\Big)\sim\frac{1}{6Q},\end{aligned} \tag{25}$$

$$2\psi\Big(\frac{3}{2}+\frac{3}{2}Q\Big)-\psi\Big(\frac{3}{2}+3Q\Big)\sim\ln 3Q-\ln 2. \tag{26}$$

From definition (22) and the above equalities, we finally get the expression of spectral index of curvature perturbation to second order:

$$\begin{aligned}n_\mathrm{s}-1=&\frac{4\eta-\frac{5}{2}\varepsilon}{1+Q}+\frac{1-\varepsilon}{2(1+Q)}\frac{\mathrm{d}\ln(T/H)}{\mathrm{d}N}\\&-\frac{\varepsilon(\eta-\frac{3}{2}\varepsilon)}{(1+Q)^2}-\frac{2+\ln 2-\gamma-\ln 3Q}{1+Q}\frac{\mathrm{d}}{\mathrm{d}N}\frac{\eta}{1+Q},\end{aligned} \tag{27}$$

where we have used the special value of Psi function $\psi(\frac{3}{2})=2-2\ln 2-\gamma$ with Euler–Mascheroni constant $\gamma=0.5772156649\cdots$. The first order of index is briefly written as

$$n_\mathrm{s}^{(1)}=1+\frac{4\eta-\frac{5}{2}\varepsilon}{1+Q}+\frac{1}{2(1+Q)}\frac{\mathrm{d}\ln(T/H)}{\mathrm{d}N}. \tag{28}$$

It is thus clear that if we get the expression of H/T, the spectral index will be determined. Next, this problem will be discussed in detail.

3. Thermodynamics of radiation field

A safe way to reheat the Universe is through the couplings of inflaton ϕ and gauge fields. Generally, the gauge boson field is regarded as the thermal bath. This model is used to explain the reheating problem in cold inflation scenario with natural and quadratic potential[22,24] and to analysis the thermal effects in warm inflation scenario,[28] then we continue the studies about inflationary thermodynamic problems in such a model. The model described by Eq. (1) shows a decay process from inflaton ϕ to thermalized $U(1)$ gauge field A_μ, in which we can calculate the energy density of radiation during inflation.

In this section, the metric is set $\mathrm{d}^2s=a^2(-\mathrm{d}^2\tau+\mathrm{d}^2x+\mathrm{d}^2y+\mathrm{d}^2z)$ with conformal time $\mathrm{d}\tau=\mathrm{d}t/a$.

3.1. Dynamical solution of gauge field

The equation of motion of 4-potential A_μ are obtained by varying the action (1) with respect to A_μ,

$$\Big[\sqrt{-g}\Big(F^{\mu\nu}+\frac{g^2\phi}{f}\tilde{F}^{\mu\nu}\Big)\Big]_{;\nu}=0, \tag{29}$$

simplified by Coulomb gauge $A_0=0$ and $\partial^iA_i=0$:

$$A_i''-a^2\partial^j\partial_jA_i-\frac{g^2a\dot{\phi}_0}{f}\eta_{ijk}\partial_jA_k=0, \tag{30}$$

with prime denoting the derivative with respect to conformal time in this section. Then decompose the gauge field A_i in terms of the annihilation and creation operators

$$\begin{aligned}A_i(\tau,\boldsymbol{x})=\sum_{\lambda=\pm}\int\frac{\mathrm{d}^3k}{(2\pi)^3}\Big[&\varepsilon_i^\lambda(\boldsymbol{k})A_\lambda(\tau,\boldsymbol{k})\hat{a}_\lambda(\boldsymbol{k})\mathrm{e}^{\mathrm{i}\boldsymbol{k}\cdot\boldsymbol{x}}\\&+\varepsilon_i^{\lambda*}(\boldsymbol{k})A_\lambda^*(\tau,\boldsymbol{k})\hat{a}_\lambda^\dagger(\boldsymbol{k})\mathrm{e}^{-\mathrm{i}\boldsymbol{k}\cdot\boldsymbol{x}}\Big],\end{aligned} \tag{31}$$

and the helicity vectors follow the relations

$$\begin{aligned}&k^i\varepsilon_i^\pm=0,\ \eta_{ijk}k^j\hat{\varepsilon}_\pm^k=\mp\mathrm{i}k\hat{\varepsilon}_i^\pm,\ \varepsilon_i^\pm\varepsilon_\pm^i=0,\ \varepsilon_i^\pm\varepsilon_\mp^i=1,\\&\sum_\lambda\varepsilon_i^\lambda(\varepsilon_j^\lambda)^*=\delta_{ij},\ \sum_\lambda\lambda\varepsilon_i^\lambda(\varepsilon_j^\lambda)^*=(\sigma_2)_{ij}=-\mathrm{i}\eta_{ij3},\end{aligned} \tag{32}$$

with σ_2 being the Pauli matrix along y direction. The annihilation and creation operators satisfy the commutation relation

$$[\hat{a}_\lambda(\boldsymbol{k}),\hat{a}_{\boldsymbol{k}'}^\dagger(\boldsymbol{k}')]=\delta_{\lambda\lambda'}\delta^{(3)}(\boldsymbol{k}-\boldsymbol{k}'). \tag{33}$$

Substituting Eq. (32) into Eq. (30) yields

$$A_\pm''+\Big(k^2\mp\frac{2k\xi}{-\tau}\Big)A_\pm=0, \tag{34}$$

where

$$\xi=g^2\dot{\phi}_0/Hf=\frac{\xi_0\varepsilon^{1/2}}{1+Q}, \tag{35}$$

with $\xi_0=3g^2M_\mathrm{p}/\sqrt{2}f$. Equation (34) is based on the assumption that the dimensionless measure of field velocity ξ evolves adiabatically, i.e., $\dot{\xi}/\xi H\ll1$. Both the solutions of positive and negative helicity modes reduce to adiabatic vacuum

at early times, i.e., $A_\pm \to \frac{e^{-ik\tau}}{\sqrt{2k}}$ as $-k\tau \to \infty$, given in terms of Coulomb functions

$$A_\pm(\tau,k) \simeq \frac{1}{\sqrt{2k}}[G_0(\pm\xi,-k\tau)+iF_0(\pm\xi,-k\tau)]. \tag{36}$$

Coulomb functions follow the asymptotic formula under the limit $\rho \to 0$:

$$F_\ell(\xi,\rho) \sim C_\ell(\xi)\rho^{\ell+1}, \tag{37a}$$

$$G_\ell(\xi,\rho) \sim \frac{\rho^{-\ell}}{(2\ell+1)C_\ell(\xi)}, \tag{37b}$$

with $C_\ell(\xi) = 2^\ell e^{-\pi\xi/2}|\Gamma(\ell+1+i\xi)|/(2\ell+1)!$. The order index in Eq. (36) is $\ell = 0$. Thus, the positive and negative helicity modes are expressed approximately as[34]

$$A_+ \sim \frac{1}{\sqrt{2k}}\left[\frac{|\Gamma(1+i\xi)|}{e^{\pi\xi/2}}(-k\tau)+i\frac{e^{\pi\xi/2}}{|\Gamma(1+i\xi)|}\right] \sim \frac{i}{\sqrt{2k}}\frac{e^{\pi\xi/2}}{|\Gamma(1+i\xi)|}, \tag{38}$$

$$A_- \sim \frac{i}{\sqrt{2k}}\frac{e^{-\pi\xi/2}}{|\Gamma(1-i\xi)|}. \tag{39}$$

3.2. Energy density of radiation field

Spatial components of electric and magnetic fields are given by

$$E_i = -\frac{1}{a^2}A_i', \quad B_i = \frac{1}{a^2}\varepsilon_{ijk}\partial_j A_k. \tag{40}$$

The energy momentum tensor of the electric and magnetic field is

$$T_{\mu\nu} = -\frac{2}{\sqrt{-g}}\frac{\delta\sqrt{-g}\mathcal{L}}{\delta g^{\mu\nu}} = g^{\alpha\beta}F_{\mu\alpha}F^{\nu\beta} - \frac{1}{4}g_{\mu\nu}F_{\alpha\beta}F^{\alpha\beta}, \tag{41}$$

with 00-component

$$\langle T_{00}\rangle = \rho_B + \rho_E = \frac{1}{2}\langle B^iB_i + E^iE_i\rangle = \frac{1}{2a^4}\langle \eta_{imk}\eta_{jnk}\partial_i A_m \partial_j A_n^* + |A'|^2\rangle. \tag{42}$$

The contraction operation represents $B^iB_i = \delta^{ij}B_iB_j$ on flat spacial coordinates due to definition (40).

The energy density could also be obtained by integrating over the momentum space:

$$\rho_B = \int d\ln k \frac{d\rho_B(k,\tau)}{d\ln k} = \int \frac{dk}{k}\frac{k^3}{(2\pi)^2}\int d^3k'\delta^{ij}\mathcal{P}_{B,ij}(\boldsymbol{k},\boldsymbol{k}',\tau). \tag{43}$$

In the above equations, $d\rho_B(k,\tau)/d\ln k$ denotes the spectral energy density of magnetic field and $\mathcal{P}_{B,ij}$ is the two-point correlation function in momentum space, with

$$\mathcal{P}_{B,ij}(\boldsymbol{k},\boldsymbol{k}',\tau) = \langle \hat{B}_i(\boldsymbol{k},\tau)\hat{B}_j(\boldsymbol{k}',\tau)\rangle = \frac{1}{a^4}\delta^3(\boldsymbol{k}-\boldsymbol{k}')\sum_{\lambda=\pm}\sum_{l_1l_2m_1m_2}\eta_{il_1m_1}\eta_{jl_2m_2}k^{l_1}k^{l_2} \times \varepsilon_\lambda^{m_1}(\varepsilon_\lambda^{m_2})^* A_\lambda(\boldsymbol{k},\eta)A_\lambda^*(\boldsymbol{k},\eta)\coth\left(\frac{k}{2aT}\right). \tag{44}$$

The hyperbolic cotangent comes from the ensemble average of creation and annihilation operators.[35] In the same way the correlation function of electric field is defined. The following equalities may be helpful to calculate the correlation functions:

$$\begin{aligned}
&\sum_{\lambda=\pm}\varepsilon_\lambda^{m_1}(\varepsilon_\lambda^{m_2})^*|A_\lambda|^2 \\
&= \sum_{\lambda=\pm}\varepsilon_\lambda^{m_1}(\varepsilon_\lambda^{m_2})^*\frac{1}{2}(|A_\lambda|^2+|A_{\bar\lambda}|^2) \\
&\quad + \sum_{\lambda=\pm}\varepsilon_\lambda^{m_1}(\varepsilon_\lambda^{m_2})^*\frac{1}{2}(|A_\lambda|^2-|A_{\bar\lambda}|^2) \\
&= \frac{1}{2}(|A_+|^2+|A_-|^2)\sum_{\lambda=\pm}\varepsilon_\lambda^{m_1}(\varepsilon_\lambda^{m_2})^* \\
&\quad + \frac{1}{2}(|A_+|^2-|A_-|^2)\sum_{\lambda=\pm}\lambda\varepsilon_\lambda^{m_1}(\varepsilon_\lambda^{m_2})^* \\
&= \frac{1}{2}(|A_+|^2+|A_-|^2)\delta^{m_1m_2} \\
&\quad + \frac{1}{2}(|A_+|^2-|A_-|^2)(\sigma_2)^{m_1m_2},
\end{aligned} \tag{45}$$

where $\bar\lambda = -\lambda$ and we have used the relations (32). Thus, two-point correlation function of magnetic field arrives at

$$\mathcal{P}_{B,ij}(\boldsymbol{k},\boldsymbol{k}',\tau) = \delta^3(\boldsymbol{k}-\boldsymbol{k}')\coth\left(\frac{k}{2aT}\right) \times [(\delta^{ij}-\hat{k}^i\hat{k}^j)k^2P_B(k,\tau) + i\eta_{ikm}\hat{k}^m k^2 S_B(k,\tau)], \tag{46}$$

where $P_B = \frac{1}{2a^4}(|A_+|^2+|A_-|^2)$ is about the symmetric part due to the nonvanishing contraction over indexes i and j, and $S_B = \frac{1}{2a^4}(|A_+|^2-|A_-|^2)$ is about the antisymmetric part with vanishing after contraction over i and j. P_B or P_E relates to the power spectrum, while S_B or S_E corresponds the polarization spectrum. Finally, the spectral energy density of magnetic field arrives at

$$\frac{d\rho_B(k,\tau)}{d\ln k} = \frac{k^3}{(2\pi)^2a^4}P_B \approx \frac{H^4}{(2\pi)^3\xi}\left(\frac{k}{aH}\right)^4(e^{2\pi\xi}+1)\coth\left(\frac{k}{2aT}\right), \tag{47}$$

where we have used the approximation[34]

$$|\Gamma(x+iy)| \sim \sqrt{2\pi}|y|^{x-(1/2)}e^{-\pi|y|/2}. \tag{48}$$

From the definition of electric field (40) and the approximations in Eqs. (37) and (48), the spectral electric density reads

$$\frac{d\rho_E(k,\tau)}{d\ln k} \approx \frac{H^4}{(2\pi)^3}\left(\frac{k}{aH}\right)^4\frac{\xi}{e^{-2\pi\xi}+1}\coth\left(\frac{k}{2aT}\right). \tag{49}$$

The numerical result shows that the magnetic spectral density is at least 10^3 times the value of electric spectral density for any value of ξ, so we can ignore the latter directly. Then the spectral density of radiation field finally arrives at

$$\frac{\mathrm{d}\rho(k,\tau)}{\mathrm{d}\ln k}=\frac{\mathrm{d}\rho_{\mathrm{B}}(k,\tau)}{\mathrm{d}\ln k}+\frac{\mathrm{d}\rho_{\mathrm{E}}(k,\tau)}{\mathrm{d}\ln k}\approx\frac{H^4}{(2\pi)^3\xi}\left(\frac{k}{k_*}\right)^4(\mathrm{e}^{2\pi\xi}+1)\coth\left(\frac{kH}{2k_*T}\right),\tag{50}$$

where k_* is the typical scale. Similarly, the spectral polarized density is

$$\begin{aligned}\frac{\mathrm{d}s(k,\tau)}{\mathrm{d}\ln k}&\approx\frac{k^5}{4\pi^2a^4}(|A_+|^2-|A_-|^2)\coth\left(\frac{k}{2aT}\right)\\&\approx\frac{H^4}{(2\pi)^2}\left(\frac{k}{aH}\right)^4\left[\frac{\mathrm{e}^{2\pi\xi}}{|\Gamma(1+\mathrm{i}\xi)|^2}-\frac{\mathrm{e}^{-2\pi\xi}}{|\Gamma(1-\mathrm{i}\xi)|^2}\right]\coth\left(\frac{k}{2aT}\right).\end{aligned}\tag{51}$$

Figure 1 plots the spectral energy density in Eq. (50) and polarized density in Eq. (51) of primordial radiation field, where the wave number k works at the typical scale $k=k_*$ and the number related to the slow-roll parameter assigns $\varepsilon^{1/2}/(1+Q)=10^{-3}$. It is found that the spectral energy density is almost independent of ξ_0 when $\xi_0<10^4$, which means that we cannot restrict the parameters of the Chern–Simons model in Eq. (1) only by the amplitude of primordial electromagnetic field. From the perspective of observational cosmology, only the observation on energy density spectrum is not enough, but also the observation on polarized density spectrum.

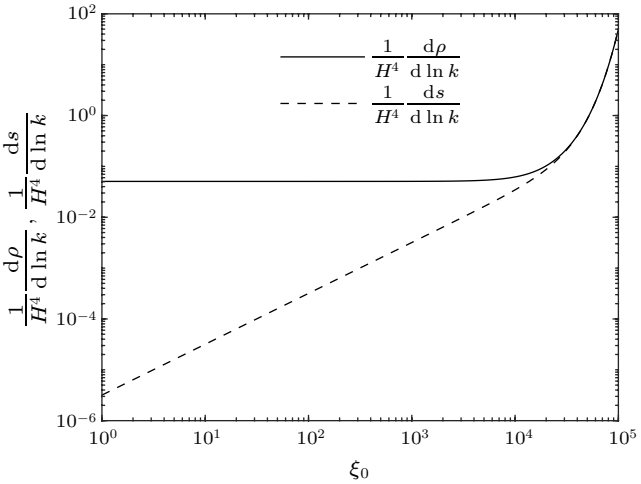


Fig. 1. The spectral energy (solid line) and polarized (dash line) density of primordial radiation field to ξ_0 by setting $k=k_*$ and $\varepsilon^{1/2}/(1+Q)=10^{-3}$.

3.3. Geometrical dynamics vs. thermal dynamics

The energy density of radiation is obtained by integrating the spectral energy density:[36]

$$\rho_{\mathrm{r}}=\int_{k_i}^{aH}\frac{\mathrm{d}k}{k}\frac{\mathrm{d}\rho(k,\tau)}{\mathrm{d}\ln k},\tag{52}$$

where $k_i\sim 0$ denotes the crossing horizon scale at the beginning of inflation. The integral containing the hyperbolic cotangent function is calculated via the series expansion method:

$$\begin{aligned}\rho_{\mathrm{r}}=\frac{H^4(\mathrm{e}^{2\pi\xi}+1)}{(2\pi)^3\xi}\Big[&\frac{1}{4}+\frac{2\pi^4}{15}\left(\frac{T}{H}\right)^4\\&+2\left(\frac{T}{H}\right)\ln(1-\mathrm{e}^{-H/T})-6\left(\frac{T}{H}\right)^2\mathrm{Li}_2(\mathrm{e}^{-H/T})\\&-12\left(\frac{T}{H}\right)^3\mathrm{Li}_3(\mathrm{e}^{-H/T})-12\left(\frac{T}{H}\right)^4\mathrm{Li}_4(\mathrm{e}^{-H/T})\Big],\end{aligned}\tag{53}$$

where we have used the integral

$$\begin{aligned}&\int_0^1x^3\coth\left(\frac{ax}{2}\right)\mathrm{d}x\\=&\int_0^1x^3\left(1+\frac{1}{\mathrm{e}^{ax}-1}\right)\mathrm{d}x\\=&\frac{1}{4}+\sum_{n=1}^{\infty}\int_0^1x^3\mathrm{e}^{-anx}\mathrm{d}x\\=&\frac{1}{4}+\sum_{n=1}^{\infty}\frac{6+[-6-6(an)-3(an)^2-(an)^3]\mathrm{e}^{-an}}{(an)^4}\end{aligned}\tag{54}$$

and $\sum_{n=1}^{\infty}n^{-4}=\pi^4/90$. Here,

$$\mathrm{Li}_s(z)=\sum_{n=1}^{\infty}\frac{z^n}{n^s}\tag{55}$$

represents the Polylogarithm functions. At the low-temperature limit, i.e., $H/T\gg 1$, the energy density of radiation is approximately

$$\rho_{\mathrm{r}}\approx\frac{H^4(\mathrm{e}^{2\pi\xi}+1)}{4(2\pi)^3\xi},\tag{56}$$

while the high-temperature limit $H/T\ll 1$ approximates to

$$\rho_{\mathrm{r}}\approx\frac{2H^3T(\mathrm{e}^{2\pi\xi}+1)}{3(2\pi)^3\xi}.\tag{57}$$

The warm inflationary scenario often works under high-temperature conditions, so Eq. (57) is used to calculate the ratio of Hubble parameter to temperature.

The energy density of radiation is also related to the temperature as

$$\rho_{\mathrm{r}}=C_{\mathrm{r}}T^4,\tag{58}$$

where $C_{\mathrm{r}}=\pi^2g_*/30$ and g_* characterizes the number of relativistic particle degrees of freedom. Combining Eqs. (58) and (57), the ratio of Hubble parameter to temperature reduces to

$$\frac{H}{T}\approx\left[\frac{2\pi^5g_*\xi}{5(\mathrm{e}^{2\pi\xi}+1)}\right]^{1/3}\approx(2\pi^5g_*/5)^{1/3}\xi^{1/3}\mathrm{e}^{-2\pi\xi/3}.\tag{59}$$

Recall the spectral index in Eq. (28). The derivative of the logarithm of T/H in Eq. (59) over e-folding number N reads

$$\frac{\mathrm{d}\ln(T/H)}{\mathrm{d}N}=-\frac{1}{3}\frac{\mathrm{d}\ln\xi}{\mathrm{d}N}+\frac{2\pi}{3}\frac{\mathrm{d}\xi}{\mathrm{d}N}=-\frac{1}{6}\frac{\mathrm{d}\ln\varepsilon}{\mathrm{d}N}$$

$$+\frac{1}{3}\frac{Q}{1+Q}\frac{\mathrm{d}\ln Q}{\mathrm{d}N}+\frac{\pi\xi_0\varepsilon^{-1/2}}{3(1+Q)}\frac{\mathrm{d}\varepsilon}{\mathrm{d}N}-\frac{2\pi\xi_0\varepsilon^{1/2}}{3(1+Q)^2}\frac{\mathrm{d}Q}{\mathrm{d}N}$$
$$\approx-\frac{1}{6}\frac{\mathrm{d}\ln\varepsilon}{\mathrm{d}N}+\frac{1}{3}\frac{Q}{1+Q}\frac{\mathrm{d}\ln(T^3/H^3)}{\mathrm{d}N}+\frac{1}{3}\frac{Q}{1+Q}\frac{\mathrm{d}\ln H^2}{\mathrm{d}N}$$
$$+\frac{\pi\xi_0\varepsilon^{-1/2}}{3(1+Q)}\frac{\mathrm{d}\varepsilon}{\mathrm{d}N}, \tag{60}$$

where we have ignored the terms higher than the second order of slow-roll parameters. Applying the slow-roll approximations in Eqs. (23a) and (23d), Eq. (60) arrives at

$$\frac{1}{1+Q}\frac{\mathrm{d}\ln(T/H)}{\mathrm{d}N}=\frac{1}{3}\frac{\eta-2\varepsilon}{1+Q}-\frac{2\pi\xi_0\varepsilon^{1/2}(\eta-2\varepsilon)}{3(1+Q)^2}. \tag{61}$$

Finally, substituting Eq. (61) into Eq.(28) and considering the strong dissipative condition $Q\gg 1$, the spectral index of curvature perturbation is briefly written as

$$n_{\mathrm{s}}^{(1)}=1+\frac{25\eta-19\varepsilon}{6(1+Q)}-\frac{\pi\xi_0\varepsilon^{1/2}(\eta-2\varepsilon)}{3(1+Q)^2}. \tag{62}$$

4. Numerical analysis of thermal dynamics

4.1. Dynamical equations and numerical estimation

In the above sections, the discussions do not involve the specific form of natural potential (6). Now we are making further discussions based on this potential.

Introduce the dimensionless variables $\mathrm{d}N=H\mathrm{d}t$, $x=\phi/f$, $y=H/M_{\mathrm{p}}$ and $z=H/T$. Then, Eqs. (2), (9) and (53) become closed equations

$$\frac{\tilde{f}^2}{2}\left(\frac{\mathrm{d}x}{\mathrm{d}N}\right)^2+\frac{\tilde{m}_\phi^2\tilde{f}^2}{y^2}(1-\cos x)+\frac{\pi^2 g_*}{30}y^2z^{-4}=3,$$
$$y^2\frac{\mathrm{d}^2x}{\mathrm{d}N^2}+y\frac{\mathrm{d}y}{\mathrm{d}N}\frac{\mathrm{d}x}{\mathrm{d}N}+3y^2(1+Q)\frac{\mathrm{d}x}{\mathrm{d}N}+\tilde{m}_\phi^2\sin x=0,$$
$$\frac{z^4}{4}+\frac{2\pi^4}{15}-12\mathrm{Li}_4(\mathrm{e}^{-z})+2z^3\ln(1-\mathrm{e}^{-z})$$
$$-6z^2\mathrm{Li}_2(\mathrm{e}^{-z})-12z\mathrm{Li}_3(\mathrm{e}^{-z})=\frac{4\pi^5 g_*\xi}{15(\mathrm{e}^{2\pi\xi}+1)}, \tag{63}$$

with $\tilde{m}_\phi=m_\phi/M_{\mathrm{p}}$, $\tilde{f}=f/M_{\mathrm{p}}$, $Q=\alpha_g\tilde{m}_\phi^3/3\tilde{f}^2y$, and $\xi=\frac{3g^2}{\sqrt{2}\tilde{f}}\frac{\varepsilon^{1/2}}{1+Q}$. The above equations may be carried out in the form of implicit differential equations.

To simulate Eq. (63), the parameters are assigned by meeting the following conditions: (1) remaining the scalar spectral index n_{s} in Eq. (62) at the moment of typical scale $k_*=0.05\ \mathrm{Mpc}^{-1}$ crossing horizon with e-folding number

$$N_*=\ln(k_*/H)\approx\ln(k_*/H(x_{\mathrm{init}})) \tag{64}$$

in tune with the current observations; (2) inflation ending with e-folding number $N_{\mathrm{end}}\approx 60$ corresponding to the condition in which the slow-roll parameter ε_H is approximately to unit, i.e., $\varepsilon_H\approx 1$; and (3) the temperature holding the order at least 10^9 GeV when the Universe entering the radiation-dominate epoch. Moreover, the potential is set as $\Lambda\sim 10^{-2}M_{\mathrm{p}}$ to ensure the Hubble expansion rate $H\sim 10^{-5}M_{\mathrm{p}}$ and $g_*=106.75$. Here the constraint from tensor-to-scalar ratio does not take into account and it will be fully used at the end of this section.

Table 1. Numerical estimation from different combinations of parameters and relevant cosmic quantities based on them.

Model	n_{s}	x_i	g	f/M_{p}	Q	$(H/T)_*$	$V_{60}^{1/4}/M_{\mathrm{p}}$	T_{eq} (GeV)
1	0.9667	-1.5042	5.551	0.10	103.6	0.3370	8.05×10^{-9}	1.21×10^{11}
2	0.9683	-1.7241	14.170	0.13	87.1	0.3302	5.89×10^{-9}	1.56×10^{10}
3	0.9693	-1.4142	30.541	0.17	84.9	0.2987	1.26×10^{-9}	4.38×10^{10}
4	0.9712	-2.1346	0.196	0.25	33.6	0.1182	4.46×10^{-9}	6.01×10^{9}

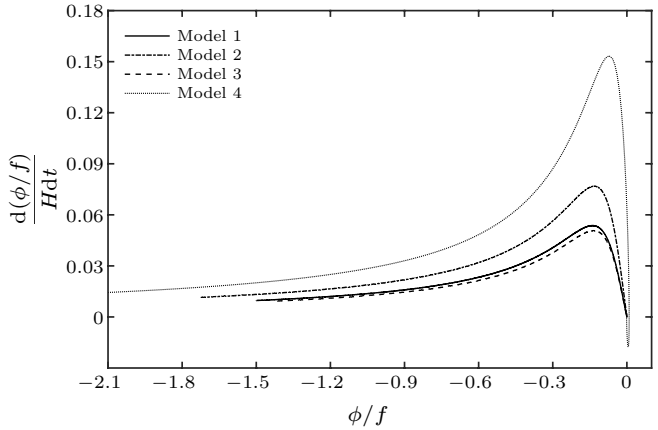


Fig. 2. Phase diagram of inflaton mean field ϕ/f and its velocity of models 1–4 listed in Table 1.

Table 1 lists four typical models satisfying the above three conditions. Model 1–3 are three typical models with strong dissipative coefficients which avoid oscillation at the potential bottom. The dissipative coefficient in model 4 is much smaller, showing an oscillation at the bottom. The phase diagrams of inflaton mean field ϕ/f and its velocity $\frac{\mathrm{d}(\phi/f)}{H\mathrm{d}t}$ are plotted in Fig. 2. Any model introduced above appears a transition from acceleration to deceleration which locates at the epoch between inflation and radiation dominating.

Figure 3 illustrates the temperature evolutions of each model mentioned above. We see that the warm inflation model avoids the reheating process and the temperature decreases gradually, which is a unique physical phenomenon of the warm inflation model.[16,28] It is also found a transition stage between inflationary epoch and radiation-dominate epoch, and the radiation-dominate epoch begins at $N\sim 70$. T_{eq} in Table 1

is the temperature at the moment of equality between potential energy and radiation energy. The model with weak dissipative coefficient (model 4) shows a temperature oscillation after inflation when the axion field moves near the potential bottom, corresponding to the oscillation of ϕ phase diagrams shown in Fig. 2. Then, Fig. 4 plots the the curves of energy density of different components. It is confirmed that the radiation-dominate epoch starts with potential $V(\phi)$ dropping below radiation energy $\rho_{\rm r}$, while the kinetic energy $\dot{\phi}^2/2$ remains always subdominant.

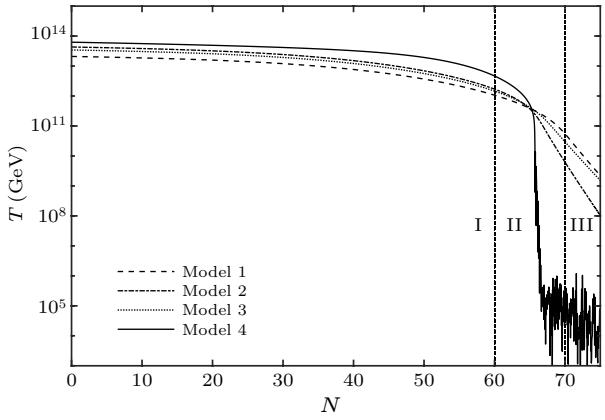


Fig. 3. Diagram of temperature T vs e-folding number N with different model. Region I denotes the inflationary epoch, region Ⅲ denotes the radiation-dominate epoch and Ⅱ means the transition epoch between them.

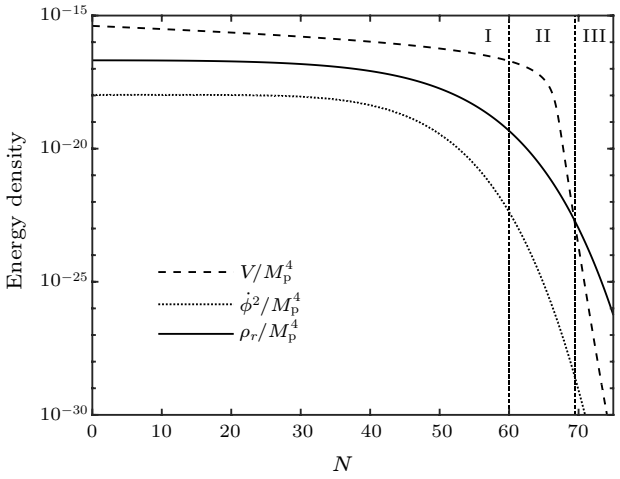


Fig. 4. The evolution of the potential, kinetic and radiation energy densities for model 1. The three regions from left to right are inflationary, transitional and radiation-dominate epoch, as the same as those in Fig. 3.

4.2. Thermodynamics

As also seen in Fig. 3, the temperature during inflation tends to a constant for any model. This result means that adiabatic approximation still holds in the warm inflationary scenario. Another interesting conclusion is that the coupling constant g has a direct effect on the behavior of temperature during inflation. As it is numerically plotted in Fig. 5, the ratio H/T is not sensitive to g if it is less than a specific value. The data H/T in Table 1 mean the values in different models. When coupling constant g is less than a threshold, H/T holds a parameter-independent constant 0.3377. In contrast, a stronger interaction constant g means a higher inflationary temperature, since a more intense conversion from vacuum potential to thermal radiation. From this perspective, radiation energy dominates the cosmic evolution when ξ (or ε) increases to a critical value. It is also well explained why the temperatures of different model have a slightly difference between each other, as shown in Fig. 3.

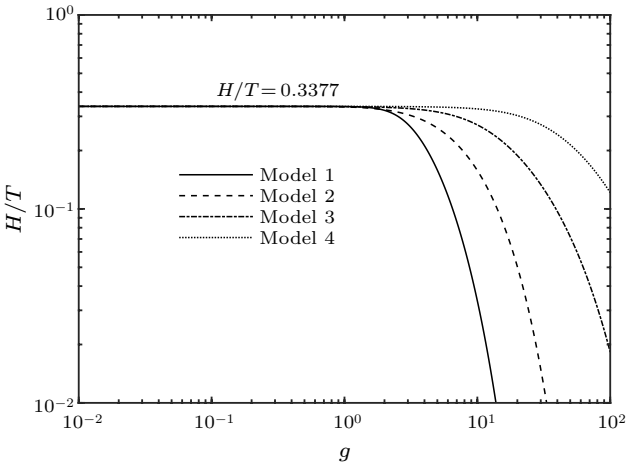


Fig. 5. Ratio of Hubble parameter to cosmic temperature H/T in terms of coupling constant g in different models.

4.3. Constrain on the parameters

Equation (63) is the accurate system of equations to simulate the thermal evolution after inflation but not convenient to constrain the relevant parameters. A concise method to constrain the parameters via the observational data is based on the slow-roll approximation. Inflation ends with $\varepsilon_{\rm H}=1$, namely,

$$x_f=\frac{1}{\bar{f}}\sqrt{\frac{2}{Q_f}}, \tag{65}$$

where $x_f=\phi_f/f$ is the dimensionless field at the end of inflation. The ratio Q at the end of inflation reads

$$Q_f=\frac{\Upsilon}{3H_f}\approx\frac{\alpha_g}{\sqrt{3}}\frac{\bar{m}_\phi^2}{\bar{f}^3\sqrt{1-\cos x_f}}. \tag{66}$$

Taylor expansion $1-\cos x\approx x^2/2$ leads to the solution of Eq. (66) as follows:[37]

$$x_f=\frac{\sqrt{24}}{\alpha_g}\frac{\bar{f}}{\bar{m}_\phi^2}. \tag{67}$$

The number of e-folding is defined as

$$\begin{aligned}N_{\rm e}&=\int_{t_i}^{t_f}H{\rm d}t\approx-\int_{\phi_i}^{\phi_f}\frac{H\Upsilon}{V_{,\phi}}{\rm d}\phi\\&=\frac{\Upsilon f}{\sqrt{3}M_{\rm p}m_\phi}\ln\tan\left(\frac{x}{4}+\frac{\pi}{4}\right)\Big|_{x_i}^{x_f}.\end{aligned} \tag{68}$$

Here, the approximation (11) with $\Upsilon \gg 3H$ and axion-like potential (6) have been used. Thus, the initial value of inflation field is obtained by solving Eq. (68),

$$x_i = -\pi + 4\arctan\left[\tan\left(\frac{x_f}{4}+\frac{\pi}{4}\right)\exp\left(-\frac{\sqrt{3}\bar{f}N_{\rm e}}{\alpha_g \bar{m}_\phi^2}\right)\right]. \quad (69)$$

Then, the value of field at horizon crossing moment x_* is approximately

$$x_* = x_i + \int_0^{N_*}\frac{\dot{\phi}}{Hf}{\rm d}N \approx x_i + \frac{\sqrt{3}\bar{f}\sin x_i}{\bar{m}_\phi^2\sqrt{1-\cos x_i}}N_*, \quad (70)$$

where N_* is introduced in Eq. (64). Substituting x_* into slow-roll parameters ε, η and Q, we can finally obtain the value of typical spectral index in Eq. (62). Another observable cosmic parameter we are interest in is the tensor-to-scalar ratio $r = \Delta_h^2/\Delta_R^2$, where Δ_h^2 has been obtained in Eq. (21) and $\Delta_h^2 = 2H^2/\pi^2 M_{\rm p}^2$ is the standard expression of vacuum tensor perturbation. Thus, we have the tensor-to-scalar ratio at typical scale crossing:

$$r = 16\frac{\varepsilon}{1+Q}\frac{Q}{1+Q}\frac{3H}{T}2^{-3+2(\alpha-\nu)} \times \frac{\Gamma^2\left(\alpha-\frac{1}{2}\right)\Gamma\left(\alpha+\nu-\frac{3}{2}\right)}{\Gamma^2(\nu)\Gamma\left(\frac{3}{2}-(\alpha-\nu)\right)\Gamma(2\alpha-2)}\bigg|_{x=x_*}. \quad (71)$$

The red narrow bands in Fig. 6 represent the 95% CL of spectral index $n_{\rm s}$ from the Planck Collaboration data[23] and the orange area in upper half represents the tensor-to-scalar ratio r within 95% CL. The dashed lines are contours of ratio H/T. The upper 95% CL band constrains the parameters with larger coupling constant, which means the non-oscillation modes after inflation epoch, as models 1–3 in Table 1. Noticeably, the lower band describes the mode with oscillation at the potential bottom, as seen in model 4. From the results in Fig. 6, it can be seen that observational data favors the non-oscillatory models, and the ratio of the Hubble parameter to cosmic temperature is estimated to be $H/T \leq 0.3377$.

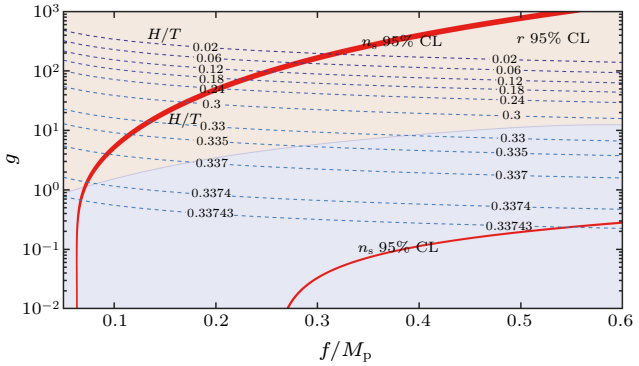


Fig. 6. Diagram of spectral index $n_{\rm s}$ and ratio H/T in terms of g and f. The red bands are the 95% CL regions of $n_{\rm s}$ from the observational data, and the dashed lines with specific value are the contours of ratio H/T. Orange area of the upper half-plane represents the 95% confidence region of tensor-to-scalar r.

5. Conclusions and outlook

In this study we introduce the model with inflaton coupling to $U(1)$ gauge field by Chern–Simons interaction and calculate its spectral index under the warm inflationary frame. Regarding the gauge field as a radiation bath, we also calculate the evolutionary trend of the ratio of Hubble parameter to cosmic temperature H/T. Lastly, numerical method is applied to analyze the relevant parameters or variables during and after inflation. By selecting the appropriate parameter combination, non-oscillating and oscillating phase diagrams are given. We find that cosmic temperature T tends to a constant during inflation and drops dramatically below the potential energy after inflation, showing a natural transition from inflation to radiation-dominant epoch. The temperature keeps a constant approximately as well during inflation meaning the adiabatic approximation still holding in warm inflation. The ratio of Hubble parameter to cosmic temperature H/T will tend to the constant 0.3377 if coupling constant is less than a threshold, being slightly dependent on relevant cosmic parameters.

Research on more complex models will be carried out in the future work. A direct idea is to calculate the spectral law of density and polarized spectrum in the model of non-Abelian axionic inflation and to test whether it can still meet the thermodynamically adiabatic phenomena shown in Figs. 3 and 5. Hence, more careful discussions on the thermal effect about warm inflation are necessary. For the rationality of the warm inflation, the conclusions obtained here need to be further verified, such as whether these conclusions can be extended to other models like reheating model with interaction $-f^2(\phi)F_{\mu\nu}F^{\mu\nu}$, whether the warm inflation model can predict the observation effects different from the cold inflation, and so on. Therefore, our next step is to have a detailed discussion on the issues raised above.

Acknowledgments

This work was supported by the National Natural Science Foundation of China (Grant Nos. 11864030 and 62061037), Inner Mongolia Natural Science Foundation (Grant Nos. 2021LHBS01001 and 2020BS02011), and the Scientific Research Funding Project for Introduced High Level Talents of IMNU (Grant No. 2020YJRC001).

References

[1] Linde A D 1983 *Phys. Lett. B* **129** 177
[2] Guth A H 1981 *Phys. Rev. D* **23** 347
[3] Linde A D 1982 *Phys. Lett. B* **108** 389
[4] Albrecht A and Steinhardt P J 1982 *Phys. Rev. Lett.* **48** 1220
[5] Hawking S W 1982 *Phys. Lett. B* **115** 295
[6] Guth A H and Pi S Y 1982 *Phys. Rev. Lett.* **49** 1110
[7] Liu X W, *et al.* 2009 *Chin. Phys. B* **18** 1362
[8] Yang J, *et al.* 2023 *Chin. Phys. Lett.* **40** 019801
[9] Ade P A R, *et al.* 2016 *Astron. Astrophys.* **594** A13
[10] Komatsu E, *et al.* 2011 *Astrophys. J. Suppl. Ser.* **192** 18

[11] An Z Y, Yue C X and Liu Z C 2018 *Chin. Phys. Lett.* **35** 061401
[12] Bastero-Gil M and Berera A 2009 *Int. J. Mod. Phys. A* **24** 2207
[13] Bartrum Sam *et al*. 2014 *Phys. Lett. B* **732** 116
[14] Bastero-Gil M, Berera A, Ramos R O and Rosa J G 2016 *Phys. Rev. Lett.* **117** 151301
[15] Arya R, Mishra A K 2022 *Physics of the Dark Universe* **37** 101116
[16] Berera A, Moss I G and Ramos R O 2009 *Rep. Prog. Phys.* **72** 026901
[17] Rammer J 2007 *Quantum Field Theory of Non-equilibrium States* (Cambridge: Cambridge University Press)
[18] Berera A, Moss I G and Ramos R O 2007 *Phys. Rev. D* **76** 083520
[19] Bartrum S, Berera A and Rosa J G 2015 *Phys. Rev. D* **91** 083540
[20] Freese K, Frieman J A and Olinto A V 1990 *Phys. Rev. Lett.* **65** 3233
[21] Ringwald A 2012 *Dark Universe* **1** 116
[22] Ferreira R Z and Notari A 2018 *Phys. Rev. D* **97** 063528
[23] Akrami Y, Arroja F, Ashdown M, *et al.* 2020 *Astron. Astrophys.* **641** A10
[24] Salvio A, Strumia A and Xue W 2014 *J. Cosmol. Astropart. Phys.* **01** 011
[25] Berghaus K V, Graham P W and Kaplan D E 2020 *J. Cosmol. Astropart. Phys.* **03** 034
[26] Das S, Goswami G and Krishnan C 2020 *Phys. Rev. D* **101** 103529
[27] Laine M and Procacci S 2021 *J. Cosmol. Astropart. Phys.* **06** 031
[28] Das S and Ramos R O 2020 *Phys. Rev. D* **102** 103522
[29] Kamali V 2019 *Phys. Rev. D* **100** 043520
[30] Barnaby N, Moxon J, Namba R, Peloso M, Shiu G and Zhou P 2012 *Phys. Rev. D* **86** 103508
[31] Berera A, Moss I G and Ramos R O 2007 *Phys. Rev. D* **76** 083520
[32] Raffelt G G 2008 *Lect. Notes Phys.* **741** 51
[33] Li X B, Zheng X G and Zhu J Y 2019 *Phys. Rev. D* **99** 043528
[34] Olver F W J, Lozier D W, Boisvert R F, *et al.* 2010 *NIST handbook of mathematical functions* (Cambridge: Cambridge University Press). From this book, we take the formulas (5.11.9), (5.15.3), (5.15.8), (10.22.57), (33.2.1), (33.2.5), (33.5.1), (33.5.2) and (33.10.2) to use in the present study.
[35] Bhattacharya K, Mohanty S and Nautiyal A 2006 *Phys. Rev. Lett.* **97** 251301
[36] Sharma R, Subramanian K and Seshadri T R 2018 *Phys. Rev. D* **97** 083503
[37] Visinelli L 2011 *J. Cosmol. Astropart. Phys.* **09** 013